Discovery and Characterization of Hydroxysteroid 17-β Dehydrogenase 13 Inhibitors

Anand Balakrishnan, Archie Reyes, Jonathan Lloyd, Manuel Roqueta-Rivera, Mary Chau, Kelsey Garlick, Yat Sun Or and Bryan Goodwin

Enanta Pharmaceuticals, Inc., 500 Arsenal Street, Watertown, MA 02472, USA.

BACKGROUND

The human *HSD17B13* gene encodes a 300 amino acid protein annotated as an NAD+-dependent 17-β hydroxysteroid dehydrogenase 13 (HSD17β13) with broad substrate specificity. Single nucleotide polymorphisms in the gene lead to reduction in full-length HSD17B13 mRNA and protein levels, and confer a strong protective effect on liver injury, inflammation, fibrosis, and cirrhosis in NASH patients. Consequently, HSD17B13 inhibitors may be beneficial in treating NASH. Here, we present the discovery of the lead series of HSD17B13 inhibitors and the elucidation of their molecular mechanisms of action using enzymology and structural biology.
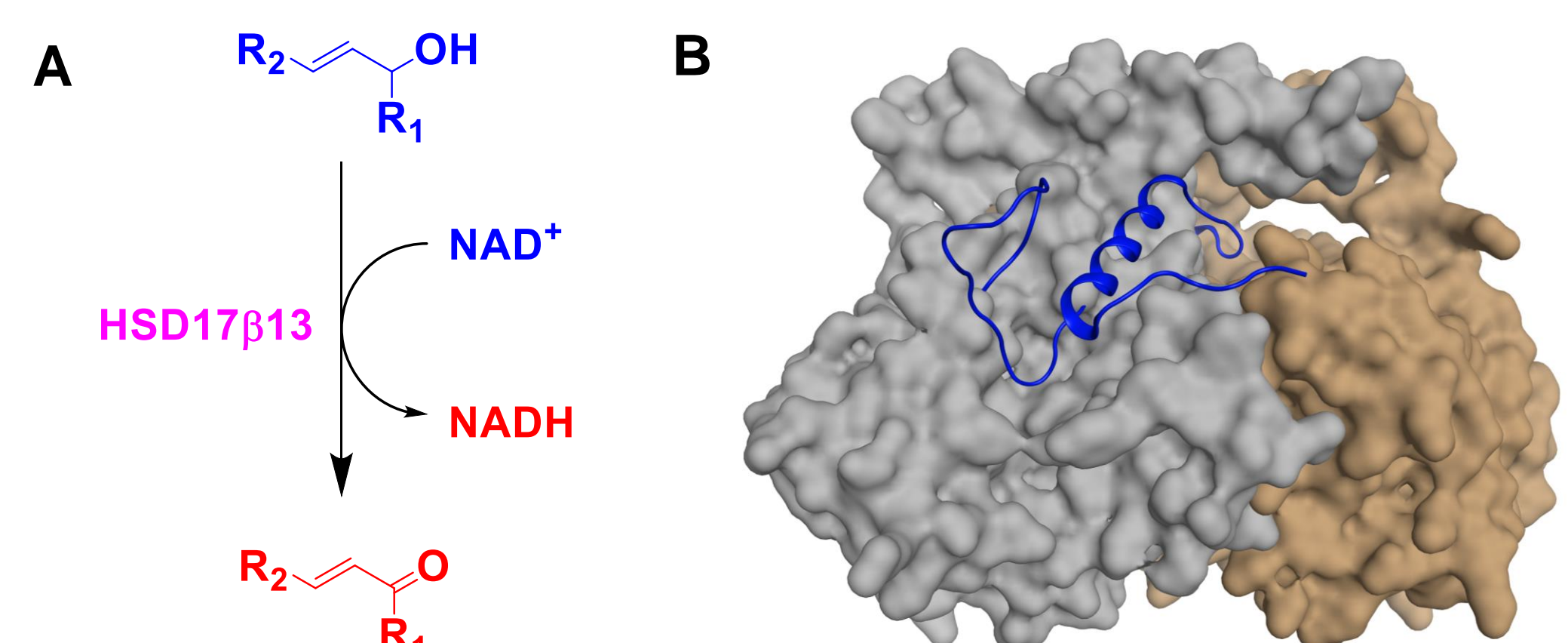
Figure 1. (A) NAD-dependent HSD17β13-catalyzed reaction, and (B) Crystal structure of dimeric HSD17β13 with mobile loops in blue

METHODS

- **Materials.** Recombinant (His)₆-ENLYFQSG- HSD17β13 was expressed in Sf9 insect cells using a baculoviral expression system and purified using metal affinity purification and size exclusion chromatography. NAD-Glo assay kit was purchased from Promega. HSD17β13 compounds were synthesized at Enanta.

- **Discovery of lead compounds against HSD17β13.** High-throughput screening to identify HSD17β13 inhibitors was performed using acoustic mass spectrometry. Hits were confirmed and characterized using coupled-enzyme luminescence assay to detect NADH and mass spectrometry assays to detect oxidized products.

- **Biochemical Assays.** Activity assays were done in 96w or 384w plates under discontinuous modes of detection: (1) chemiluminescence from the NAD-Glo assay; and (2) product detection via RapidFire mass spectrometry. Assay mixtures contained 40 mM Tris (pH 7.4), 0.01% BSA, 0.01% Tween 20, 50-100 nM enzyme, 10 - 50 μM substrates (LTB4/estradiol), and 0-100 μM compounds.

- **Structural Analysis.** Structure determination using x-ray crystallography was performed with HSD17β13 co-crystallized in the presence of inhibitors and/or NAD+.

RESULTS

❑ Discovery of HSD17β13 Inhibitors

- From 502 HTS hits , we have identified 4 lead series that were reconfirmed for their potencies and HSD selectivity via luminescence-NADH assay and RF/MS analysis. Further structural analyses led to Series 1c, 2b and 2c compounds.

RESULTS

❑ HTS produced hit clusters with multiple hits
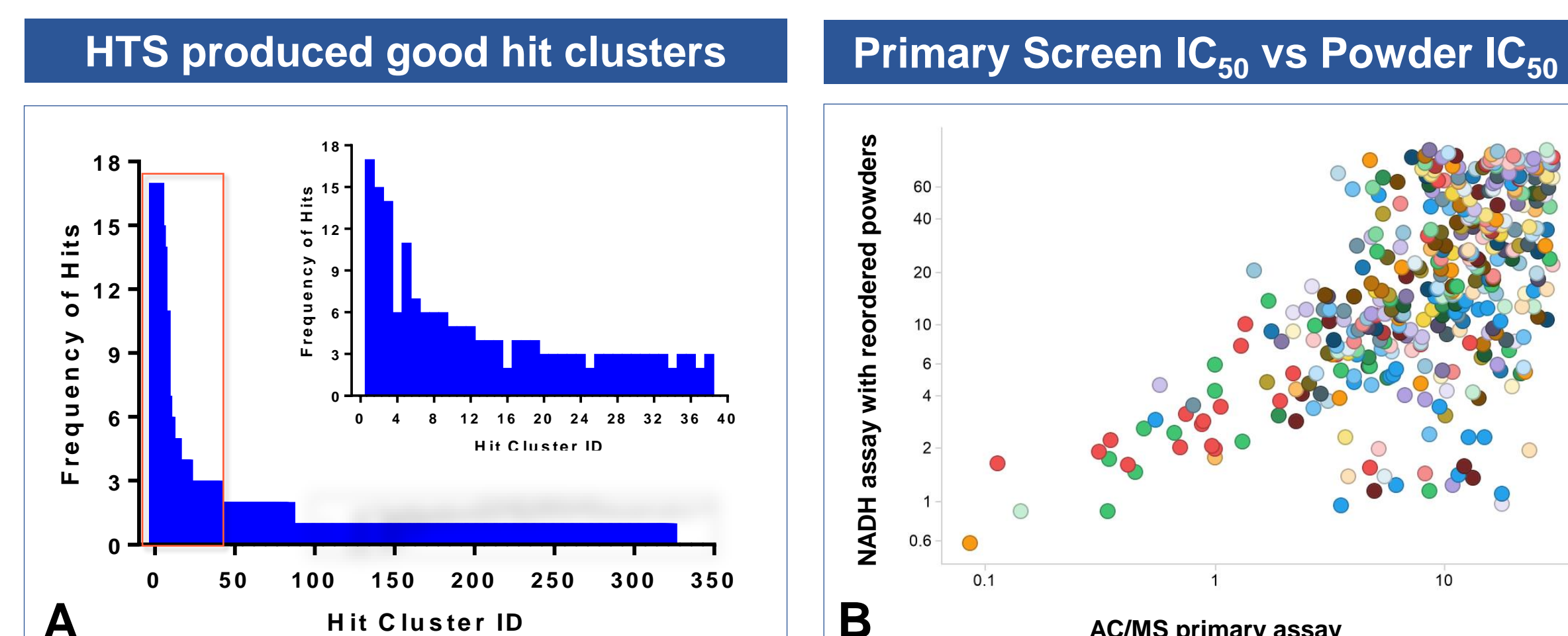
Figure 2. (A) Hit clustering of 502 compounds from HTS, and (B) Reconfirmation of hits via Luminescence-NADH assay and MS analysis

❑ Multiple hits showed good selectivity to other HSD17βXs

20 compounds passed criteria of Selectivity Index > 20

Reconfirmed in RapidFire mass spectrometry assays

No activity in Estrogen receptor assays at up to 20 μM

Synthetic tractability and IP analysis.

4 lead compounds were selected for further studies (Series 1a, 1b, 2a, 3)
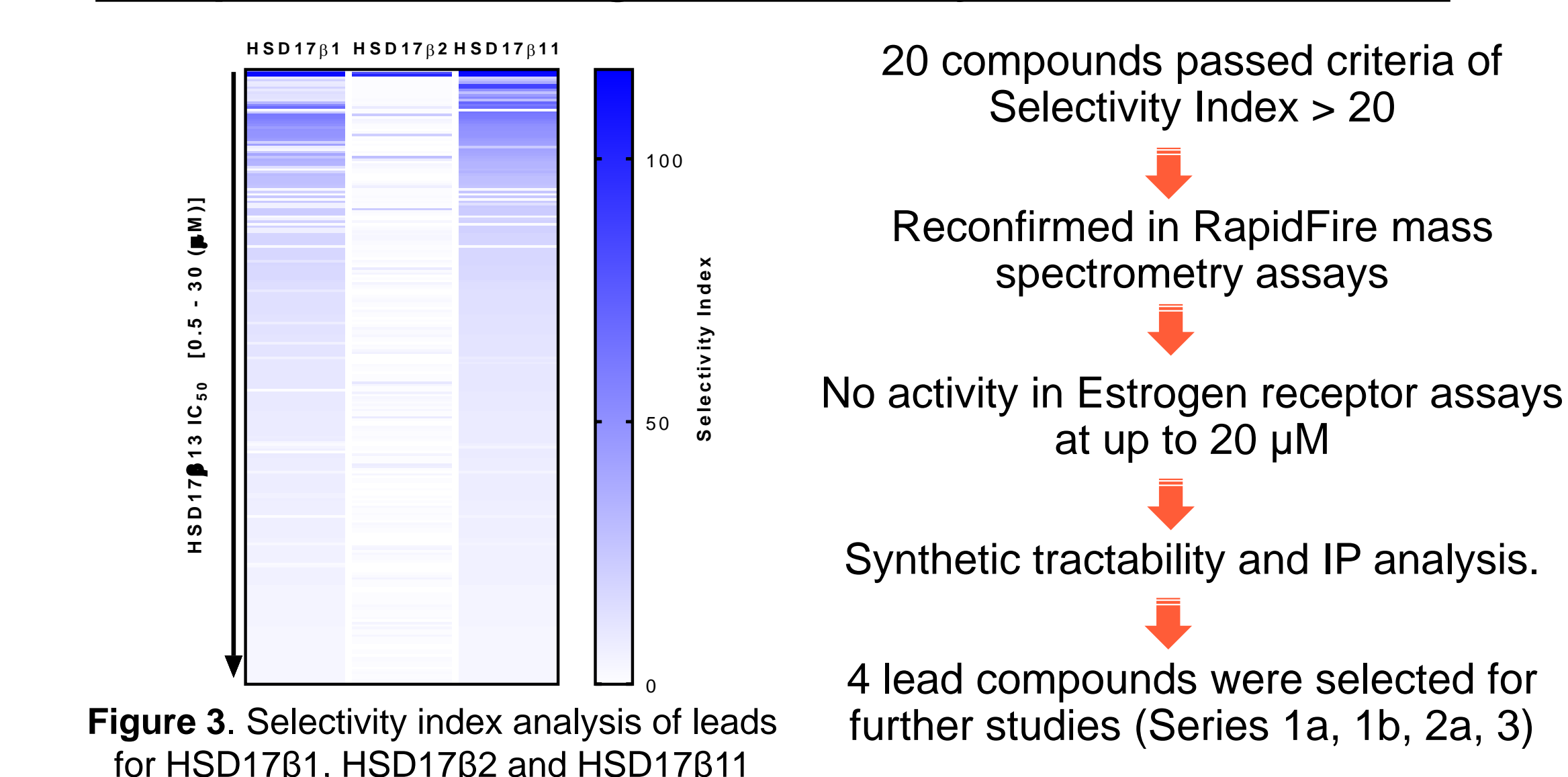
Figure 3. Selectivity index analysis of leads for HSD17β1, HSD17β2 and HSD17β11

❑ First series of HSD17β13 compounds are non-competitive

Table 1. HSD17β13 inhibition modality by the series 1, 2a and 3 compounds. IC₅₀ = half-maximal inhibitory concentration, K_i = inhibition constant and α = inhibitor affinity index.

Series	IC₅₀ (μM)	Constant	Varied	Model	K_i (μM)	αK_i (μM)
1a	0.25	NAD+	LTB4	Non-competitive	0.166	1.18
		LTB4	NAD+	Non-competitive	0.30	0.30
1b	0.014	NAD+	LTB4	Non-competitive	0.0214	0.0214
		LTB4	NAD+	Non-competitive	0.010	0.022
2a	0.055	NAD+	LTB4	Non-competitive	0.0176	0.0738
		LTB4	NAD+	Non-competitive	0.045	0.027
3	0.04	NAD+	LTB4	Non-competitive	0.0446	0.222
		LTB4	NAD+	Non-competitive	0.068	0.136

❑ Structural biology of HSD17β13 enables lead optimization

X-ray crystallography revealed dynamic regions near the active site

Lead optimization: Series 1c, 2b, 2c
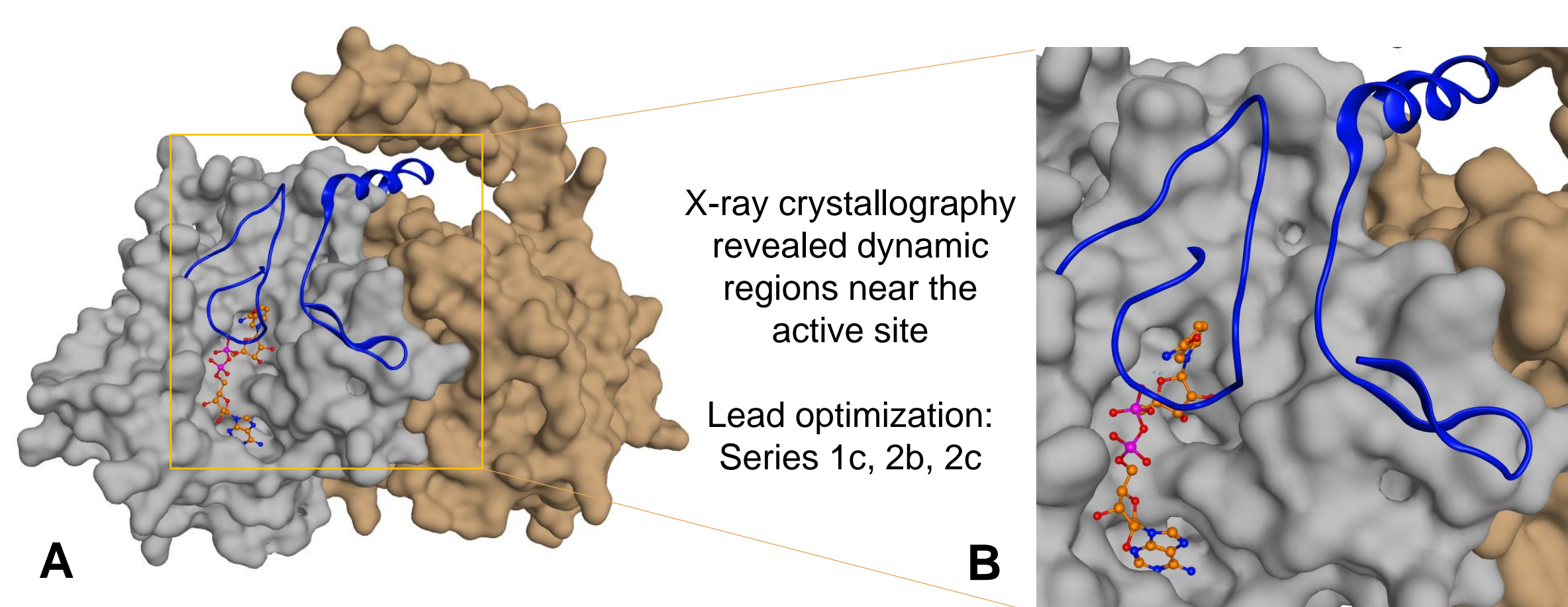
Figure 4. (A) Crystal structure of dimeric NAD-bound HSD17β13, and (B) Zoomed-in substrate binding site of HSD17β13 showing the NAD-binding loop and the mobile C-terminus (both in blue)

RESULTS

❑ Potent and selective inhibition of HSD17β13 series 1 and 2

Table 2. Potency and selectivity of HSD17β13 Series 1c, 2b and 2c compounds.
[1]RF/MS= Rapid Fire Mass Spectrometry with Leukotriene B4; [2]RF/MS= RapidFire Mass Spectrometry with E2=Estradiol; [3]NADH Luminescence Assay; [4]Direct measurement of NADH consumption at 340 nm.

Assay		1c	2b	2c
Biochemical Activity[1,2] Inhibition of product formation (RF/MS)	Human[1], IC₅₀	14 nM	79 nM	37 nM
	Mouse[2], IC₅₀	2.5 nM	74 nM	9 nM
Cellular Activity[2] Inhibition of product formation (RF/MS)	HEK293 Human, IC₅₀	47 nM	34 nM	28 nM
	HEK293 Mouse, IC₅₀	55 nM	1083 nM	45 nM
HSD Selectivity[3] IC₅₀ ratio (HSD17βx/ HSD17β13)	HSD17B1	>7000×	>1265×	1838×
	HSD17B2	4357×	322×	322×
	HSD17B4	>7000×	982×	1260×
	HSD17B3, B5, B10, B11	>7000×	>1265×	>2700×
	HSD11B1	>7000×	>630×	>1350×
DH Selectivity IC₅₀ ratio (Metabolic DH/ HSD17β13)	Human isocitrate dehydrogenase 1[3]	>7000×	>1265×	>2700×
	Rabbit glycerol-3-P dehydrogogenase[4]	4285×	150×	170×
	Rabbit lactate dehydrogenase[4]	>7000×	>1265×	190×

❑ HSD17β13 series 1c, 2b and 2c are tight-binding inhibitors

	K^{app} (nM)
1c	4.1 ± 0.4
2b	90 ± 19
2c	16 ± 2
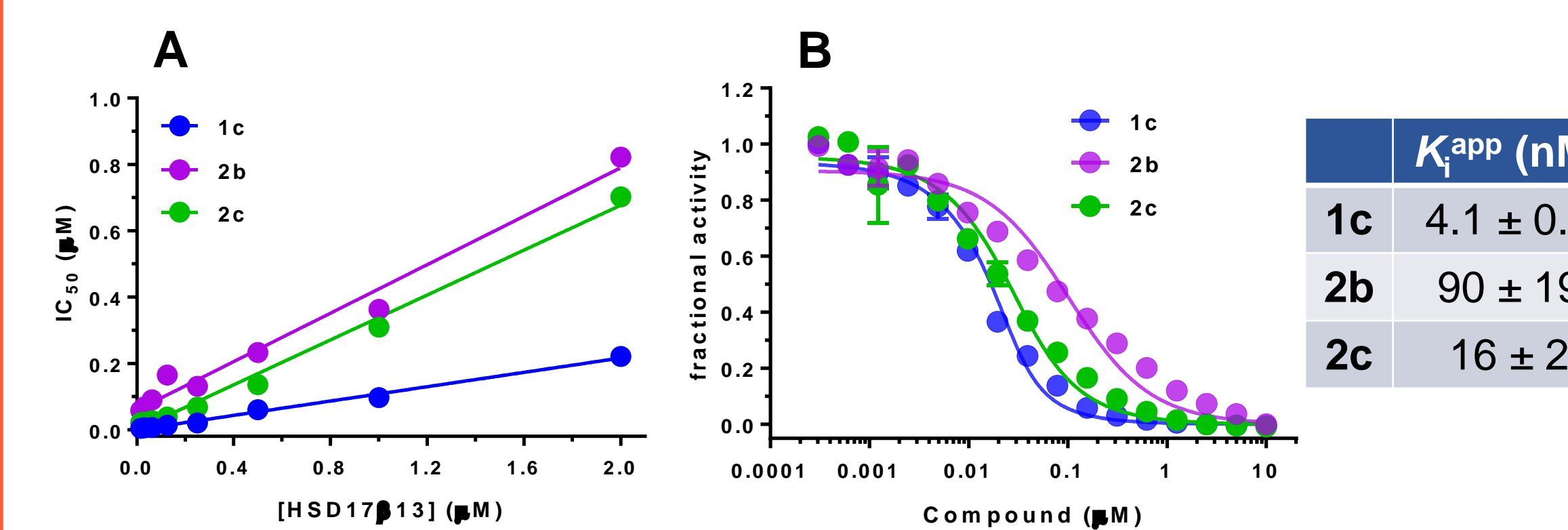
Figure 5. (A) Dependence of IC₅₀ on HSD17β13 concentration; and (B) Morrison Fit analysis for tight binding inhibition. IC₅₀ = half-maximal inhibitory concentration, K^{app} = apparent inhibition constant. Data are mean ± standard deviation of duplicates.

❑ Progress curves studies suggest rapid onset inhibition
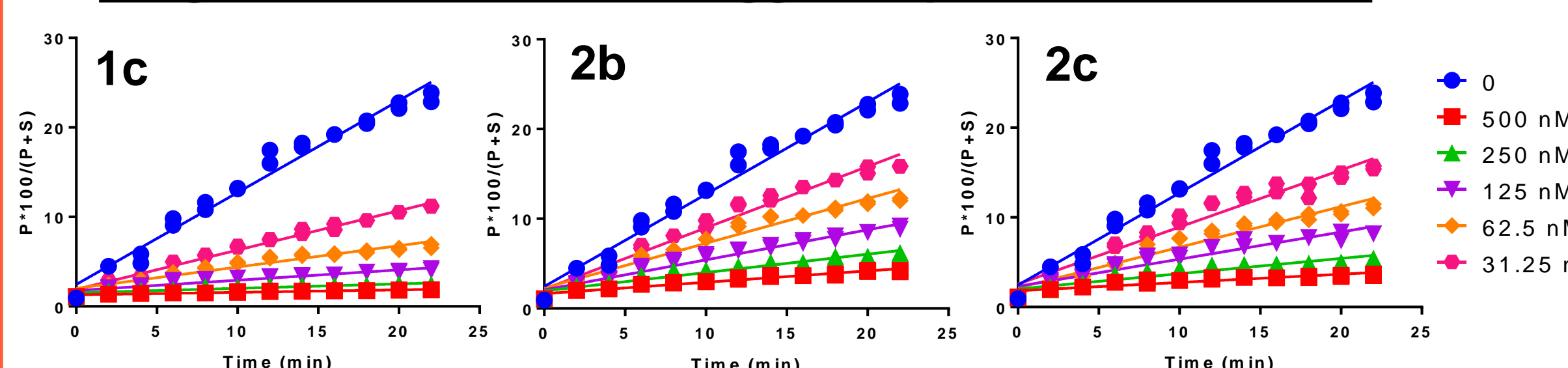
Figure 6. Linear progress curves in presence of various concentrations of HSD17β13.

❑ HSD17β13 series 1c, 2b and 2c are reversible inhibitors

Jump Dilution Experiment

Preincubate enzyme with inhibitor → 100x dilution into substrate solution → End point product

Source Plate → Assay Plate
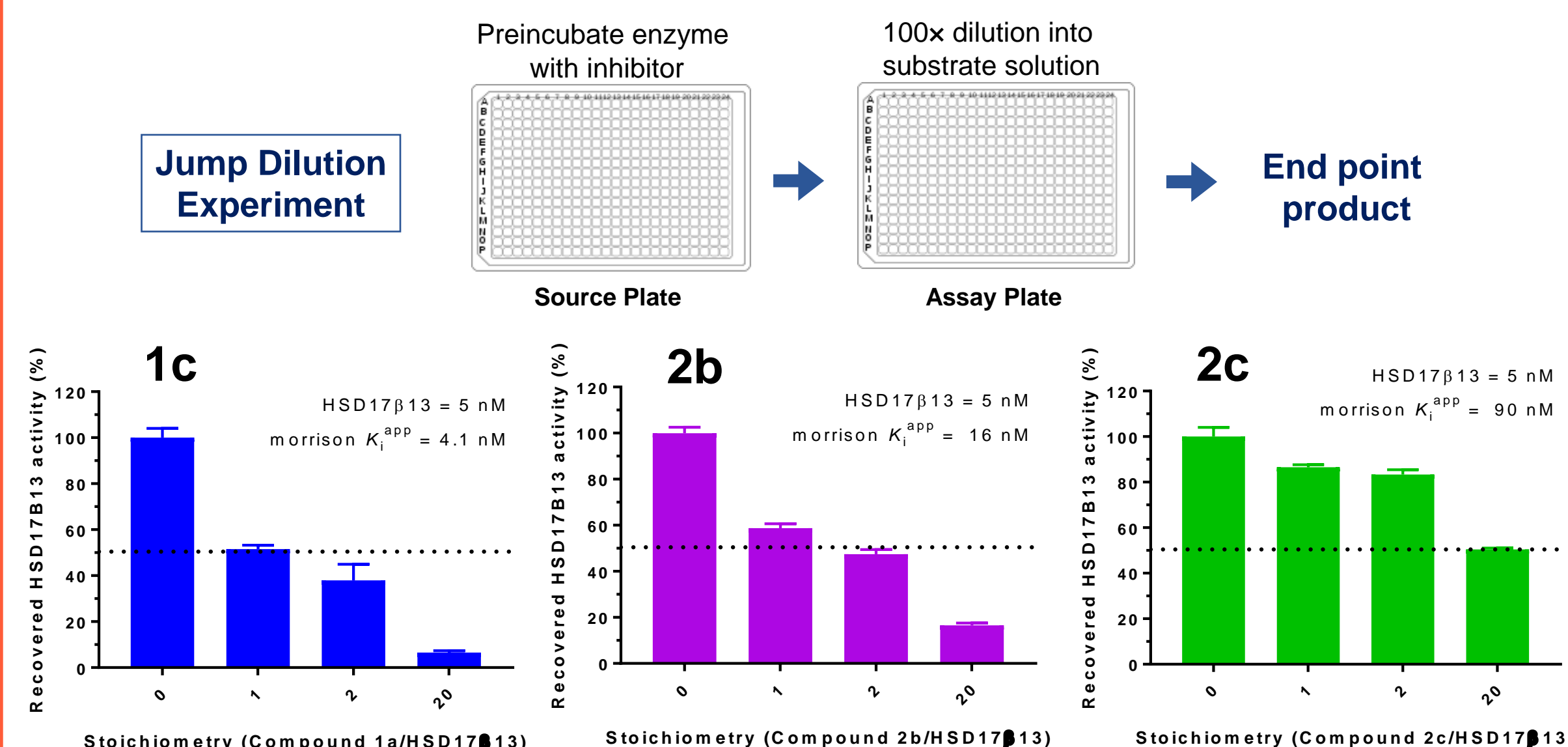
Figure 7. Jump dilution reversibility test for HSD17β13 inhibition by lead candidates. Data are mean ± standard deviation of triplicates.

RESULTS

❑ HSD17β13 series 1c, 2b and 2c are non-competitive
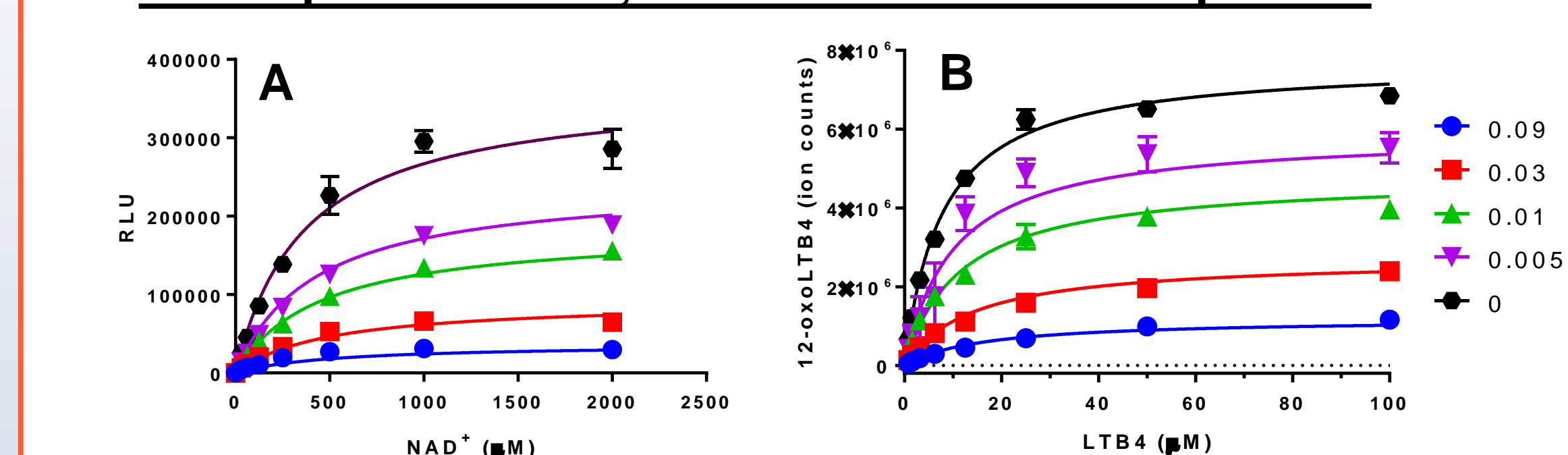
Figure 8. Series 2c is a noncompetitive HSD17β13 inhibitor with respect to (A) NAD+ and (B) LTB4.

Table 3. HSD17β13 inhibition modality by Series 1c, 2b and 2c. IC₅₀ = half-maximal inhibitory concentration, K_i = inhibition constant and α = inhibitor affinity index. Data are mean ± standard deviation of triplicates.

	Varied NAD+			Varied LTB4		
	K_i (nM)	α	Model	K_i (nM)	α	Model
1c	5 ± 0.2	0.7 ± 0.2	Non-competitive	1.7 ± 0.1	11 ± 2	Non-competitive
2b	135 ± 26	0.7 ± 0.1	Non-competitive	25 ± 14	13 ± 2	Non-competitive
2c	9 ± 3	1.3 ± 0.4	Non-competitive	7.2 ± 0.1	2.2 ± 0.2	Non-competitive

❑ Lead optimized compounds binding at the HSD17β13 active site induces conformational changes in the dynamic regions
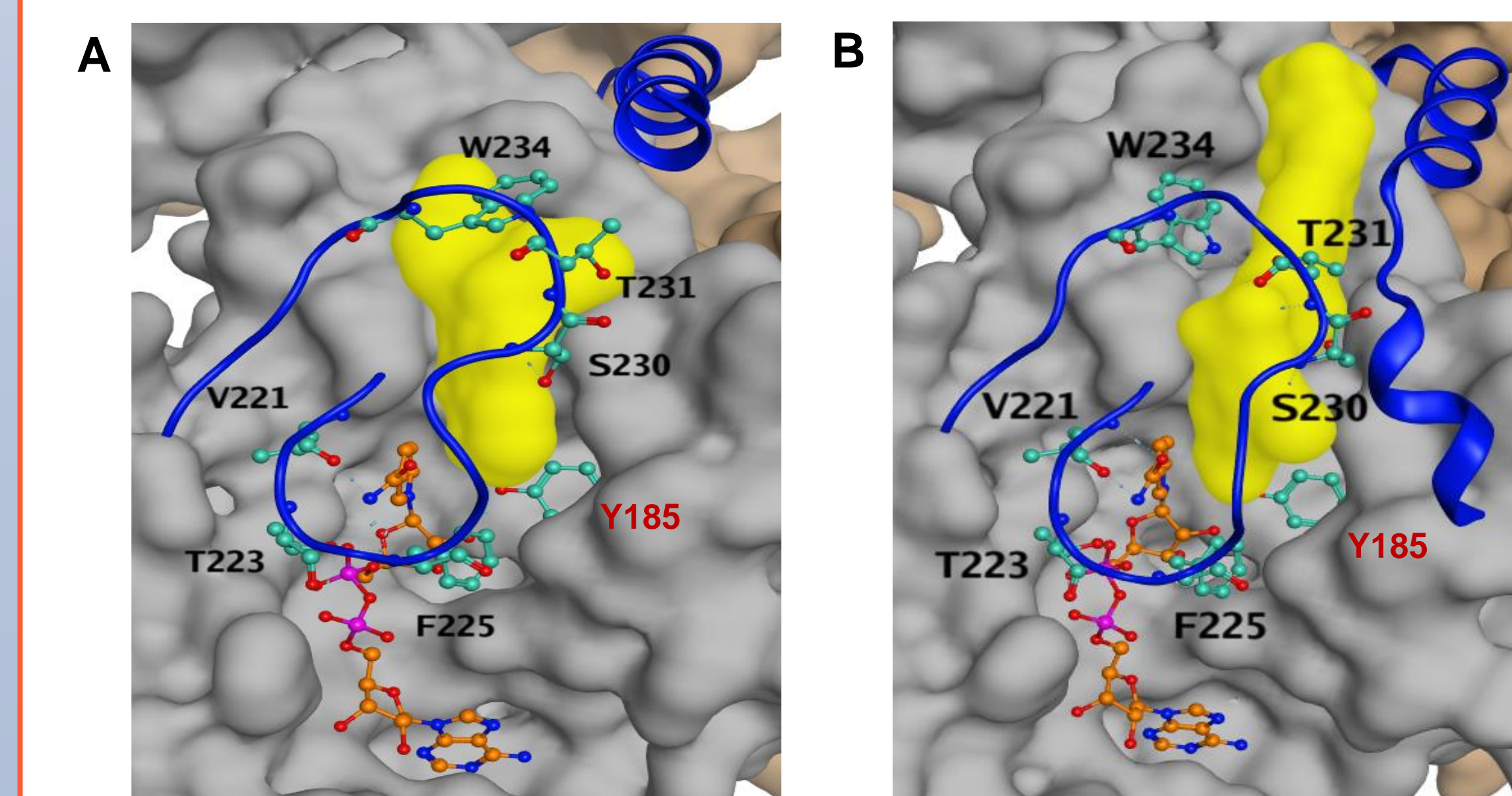
Figure 9. Series 2 compounds 1c (A) and 2b (B) induce conformational changes in HSD17β13. NAD-binding loop and the mobile C-terminus are shown in blue. Residues involved in NAD interactions: V221, T223 and F225. Residues involved in inhibitor interactions: S230, T231 and W234.

CONCLUSION

- Biochemical characterization of HSD17B13 and the development of specific inhibitors will enable a deeper understanding of the pathophysiological function of this enzyme in chronic liver disease.

- We have identified HSD17B13-specific inhibitors and utilized these compounds to probe the enzymology and structural biology of HSD17B13.

- Crystallographic structures of HSD17B13 in complex with substrates/inhibitors shed light on the catalytic function and inhibition of this enzyme.

ACKNOWLEDGEMENTS